Journal of NUCLEAR SCIENCE and TECHNOLOGY, Vol. 44, No. 2, p. 109–113 (2007)

ARTICLE

A Correction Factor for Effects of Scattered X-rays at Calibration of Ionization Chambers in Low Energy X-ray Standard Fields

Akihiro NOHTOMI[1,*], Nobuhisa TAKATA[1] and Takeji SAKAE[2]

[1]*National Institute of Advanced Industrial Science and Technology (AIST), NMIJ, 1-1-1 Umezono, Tsukuba-shi, Ibaraki 305-8568, Japan*

[2]*Proton Medical Research Center (PMRC), University of Tsukuba, 1-1-1 Ten-nohdai, Tsukuba-shi, Ibaraki 305-8575, Japan*

(Received April 13, 2006 and accepted in revised form October 28, 2006)**

A correction factor k_s is related to contributions of scattered photons at calibration in standard X-ray fields. We obtained values of k_s for spherical and parallel-plate ionization chambers in low energy X-ray fields experimentally. Signal currents from these chambers were measured using copper plate collimators with different diameter holes to vary the field size. To derive k_s values, the measured data were analyzed using a simple model. It was found that the value of k_s increases with the increase of the effective energy of X-rays.

KEYWORDS: soft X-ray, standard field, calibration, ionization chamber, field size, outer scattering, correction factor

I. Introduction

The dosimetry of low energy X-rays, which are generated using an X-ray tube at tube voltages between 10 to 50 kV, has been of growing importance due to the proliferation of various appliances using X-rays. For example, mammographic devices have been introduced in many hospitals in Japan and it is required to estimate the dose to patients during diagnosis because excessive or unnecessary exposure should be avoided. For this purpose, appropriate X-ray detectors, generally ionization chambers, are routinely used, and it is important that they should be calibrated using standard X-ray fields.

Free-air ionization chambers (FACs) have been used to determine the absolute value of the dose in standard X-ray fields.[1,2] In an X-ray field, there are photons scattered by the collimator, filter and ambient air as well as photons emitted directly from the X-ray tube. The various varieties of ionization chambers have different sensitivities to these scattered photons because the photons are incident over a wide range of angles. Free-air ionization chambers, which typically have a thick diaphragm as an aperture for confining the X-ray beam, are expected to have relatively low sensitivities to these scattered photons. Consequently, when calibrating ionization chambers, it is necessary to take into account the differences between the sensitivity of free-air ionization chambers and that of ionization chambers for scattered photons which are calibrated. However, such differences are generally ignored even for medium energy X-rays.

The dependence of ionization chamber response on field-diameter has been observed and it has been noted that this effect should be taken into account at calibration.[3,4] In this article, the effects of scattered X-rays on the responses of spherical, parallel-plate and free-air ionization chambers are measured and the correction factor, k_s, for calibration of spherical and parallel-plate ionization chambers are investigated. As a first approximation, it was assumed that all scattered photons are generated through the interaction with surrounding ambient air between the collimator and ionization chambers. Other all components have not be considered for simplicity, such as the edge scattering by the collimator and the reflection by the room wall and floor.

II. Experiment

Experiments were carried out for the low-energy X-ray primary standard fields at NMIJ/AIST in Japan. A spherical ionization chamber (Shonka–Wyckoff A3) and a parallel-plate ionization chamber (PTW 23344) were placed at 1 m from an X-ray source. The outer diameter of the A3 chamber was 19 mm, the wall thickness of the chamber was 0.25 mm and the sensitive volume was 3.6 cm^3. The reference point for the A3 chamber was chosen to be the center of the sphere. The sensitive region of the PTW chamber had a diameter of 13 mm, while the entrance foil of the chamber was 0.03 mm-thick mylar and the sensitive volume was 0.2 cm^3. The reference point for the PTW chamber was chosen to be the surface of the entrance window.

The signal outputs from a chamber were measured with and without four 5 mm-thick copper plate at the midway between the X-ray source and the ionization chamber. Therefore, the radiation field size at the reference point became just twice of the collimator hole diameter. The hole diameters were 15, 20, 30 and 40 mm (**Fig. 1**). The collimator was sufficiently thick to prevent X-ray penetration. The collimator plate size was large enough (300 mm × 300 mm) to prevent injection of scattered photons that occur between the X-ray source and the collimator. These collimators are not used when actual calibration is performed. The scattered

*Corresponding author, E-mail: a-nohtomi@aist.go.jp

**This article was received and accepted as "Original Paper".

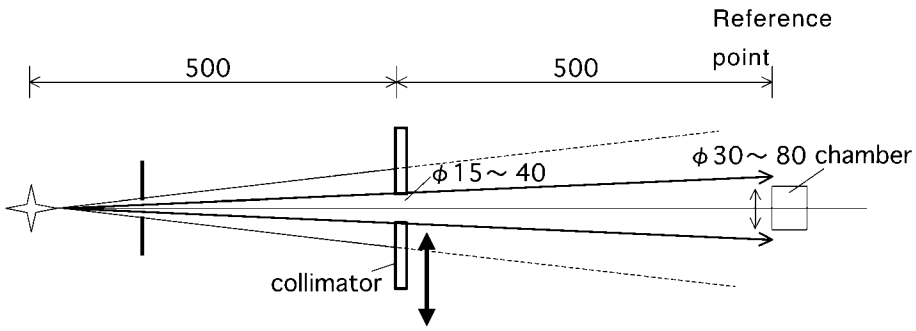

Fig. 1 Experimental set up for the evaluation of the scattered photon contribution
Values are in mm.

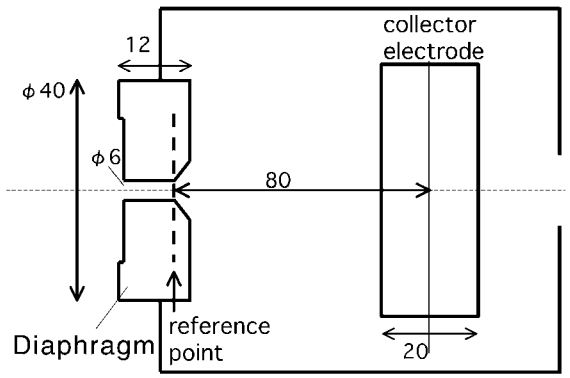

Fig. 2 Schematic drawing of the free-air ionization chamber
Dimensions are in mm.

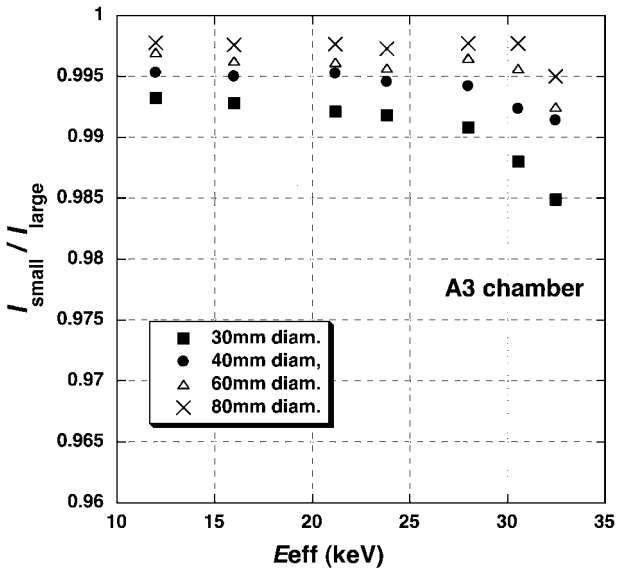

Fig. 3 The dependence of I_{small}/I_{large} on E_{eff} with different field sizes for an A3 chamber

photons by the room wall and floor can be neglected because the height of the X-ray beam was about 1.5 m from the floor and the room was wide enough.

The diameter of the X-ray field at the reference point was 150 mm when no copper collimator was inserted. The change in the signal current with and without the collimators can therefore be attributed to scattered photons that were blocked by the collimator. Similar measurements using the same collimators were also made for a free-air ionization chamber for low-energy X-rays. The FAC had a 12 mm-thick tungsten diaphragm with a six mm diameter aperture. The distance from the reference point to the center of the charge collector electrode was 80 mm (**Fig. 2**).

III. Measurement Results and Analysis

1. Measurement

Measurements were made for various effective energies (E_{eff}) in the range from 12 to 32.5 keV, with tube voltages of 15–50 kV and with field diameters of 30, 40, 60 and 80 mm at the chamber position. The tube current of the X-ray generator was typically 30 mA and the stability of the output was better than ±0.1%/h. The results are shown in **Figs. 3**, **4** and **5**, where I_{small} is the current obtained with a copper collimator, and I_{large} is that obtained without the collimator. The ratio I_{small}/I_{large} (referred to as f later on) is plotted as a function of E_{eff} in the respective figures. The figures show that the value of f decreases as E_{eff}

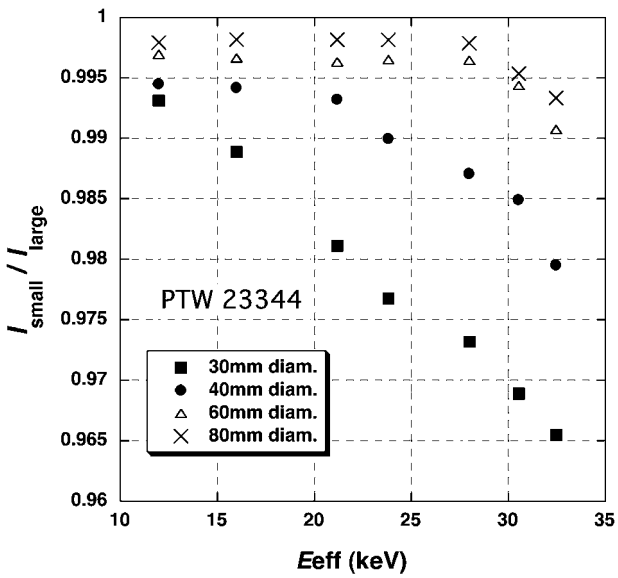

Fig. 4 The dependence of I_{small}/I_{large} on E_{eff} with different field sizes for a PTW chamber

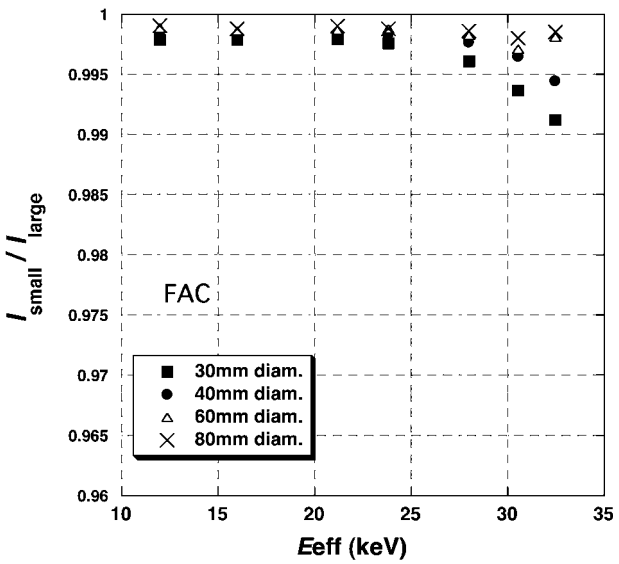

Fig. 5 The dependence of I_{small}/I_{large} on E_{eff} with different field sizes for FAC

increases for all three of the ionization chambers. But in Fig. 4 (PTW chamber), the values of f for 30 mm diameter and 40 mm diameter show sharp decreases and are apparently different from the results for other diameters. The reason for the sharp decreases is studied later in the Chapter for discussion. However, the results for 30 and 40 mm diameters are omitted from the present data analysis.

2. Evaluation of Correction Factor Based on a Modeling

We propose a simple model to derive the correction factors, k_s, from the data obtained. It is assumed that the contribution of scattered photons is proportional to the effective interaction volume of ambient air. The constant of proportionality is taken to be a and the model is derived as follows. The value B^G for PTW and A3 chambers is the ratio between the net signal current I_{net}, which excludes any contribution due to scattered photons and I_{small} which is the measured current for a certain field size:

$$B^G = \frac{I_{net}}{I_{small}}. \tag{1}$$

We would like to know this factor for the large field size, B^G_{large}. The value of I_{large} is the measured current without a collimator, which corresponds to a field size of 150 mm. Consequently, I_{large} and I_{small} are expressed as the sum of I_{net} and a term which corresponds to the effect of scattered photons:

$$\begin{cases} I_{large} = I_{net} + a\pi(r_3^2 - r_1^2) \\ I_{small} = I_{net} + a\pi(r_2^2 - r_1^2) \end{cases}, \tag{2}$$

where r_1 is the radius of each chamber (9.5 mm for A3 and 6.5 mm for PTW), r_2 is the radius of the X-ray field at the chambers with copper collimators (15, 20, 30, 40 mm) and r_3 is the radius of the field diameter without a collimator (75 mm in all cases treated in this study). The relation between these values are shown in **Fig. 6**.

Here, it should be noted that $\pi(r_3^2 - r_1^2)$ and $\pi(r_2^2 - r_1^2)$ are proportional to the ambient air volume which causes scattered photons because the volume of a cone shape is proportional to the area size of its base when the height is the same. The value f, ratio of I_{small} to I_{large}, and the geometrical factor Y is introduced as:

$$f = \frac{I_{small}}{I_{large}}. \tag{3}$$

$$Y = \frac{r_3^2 - r_1^2}{r_2^2 - r_1^2}. \tag{4}$$

From Eqs. (1)–(4), the correction coefficient B^G for each chamber can finally be written as:

$$B^G = \frac{Y - I_{large}/I_{small}}{Y - 1} = \frac{Y - 1/f}{Y - 1}. \tag{5}$$

The values of B^G_{large} for the field size of 150 mm were obtained by plotting the experimental results, B^G, as a function of the field diameter and fitting a quadratic function with them. Those values were then determined by extrapolating the fitted function up to 150 mm. As an example, the result for 21.2 keV is shown in **Fig. 7**. In the fitting of a curve for all chambers, the data points for the field diameters of 30 and 40 mm were omitted. This was because when the data point was included it was not possible to obtain a good fit with a quadratic function.

The value B^{FAC}_{large}, which is for FAC, was not obtained using

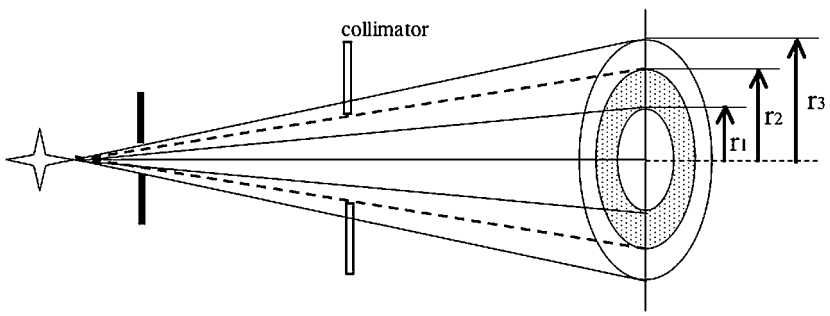

Fig. 6 Geometry of the modeling

Notations are r_1: chamber radius (9.5 mm for A3, 6.5 mm for PTW and 3 mm for FAC), r_2: radiation field radius at the chamber (15, 20, 30 and 40 mm) and r_3: maximum radiation field radius at the chambers with no collimator (75 mm).

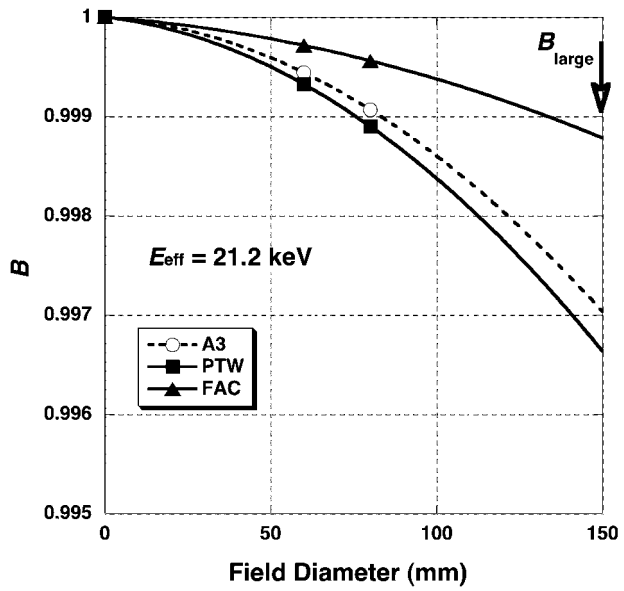

Fig. 7 The dependence of the value B on field size when E_{eff} is 21.2 keV

The data points of the field diameter of 30 and 40 mm for all chambers have been omitted.

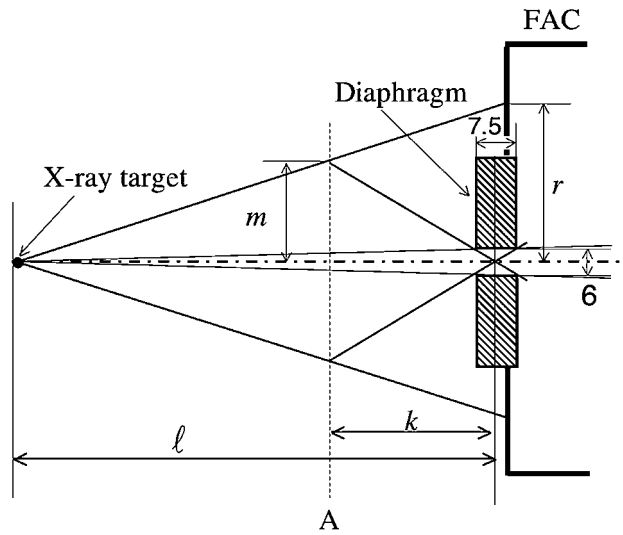

Fig. 8 Detailed geometry which was used for the evaluation of FAC effective interaction volume

The unit of the length is mm.

above way because the structure of FAC was different from other chambers as shown in Fig. 2; the distance between the reference point and the centre of collector electrode is 80 mm and the acceptance for incident photons is significantly limited by the diaphragm geometry used. We introduce an effective interaction volume (V_{eff}) to evaluate $B^{\mathrm{FAC}}_{\mathrm{large}}$.

By referring **Fig. 8**, the effective interaction volume V_{eff} is expressed as follows,

$$V_{\mathrm{eff}} = V_1 + V_2 - V_3, \tag{6}$$

where the V_1 denotes the volume of the left side cone from the plane A and V_2 denotes that of the right side cone from the plane A. The V_3 denotes the volume of an inner cone of the aperture whose height is ℓ, *i.e.* 1,000 mm, and the radius of the base circle is 3 mm. Therefore,

$$V_1 = \frac{\pi m^2(\ell - k)}{3}, \quad V_2 = \frac{\pi m^2 k}{3} \text{ and } V_3 = \frac{\pi 3^2 \ell}{3}. \tag{7}$$

$$V_{\mathrm{eff}} = \frac{\pi \ell}{3}(m^2 - 9). \tag{8}$$

Moreover, there are some relations between m and k,

$$m = \frac{r}{\ell}(\ell - k), \tag{9}$$

$$k = \frac{7.5}{6} m. \tag{10}$$

Consequently, m is expressed as a function of the field size r as follows,

$$m(r) = \frac{r}{1 + \frac{7.5}{6\ell} r}. \tag{11}$$

In a similar procedure of the derivation of Eq. (5), I_{small} and I_{large} for FAC are expressed as follows,

$$\begin{cases} I_{\mathrm{large}} = I_{\mathrm{net}} + \dfrac{\ell \pi b}{3}[m(r_3)^2 - 9] \\ I_{\mathrm{small}} = I_{\mathrm{net}} + \dfrac{\ell \pi b}{3}[m(r_2)^2 - 9] \end{cases}, \tag{12}$$

here, b denotes the constant of proportionality between the number of scattering photons and the effective interaction volume of air, which is similar to Eq. (2).

$$Y' \equiv \frac{m(r_3)^2 - 9}{m(r_2)^2 - 9}. \tag{13}$$

Then, correction factor B^{FAC} for FAC is expressed as:

$$B^{\mathrm{FAC}} = \frac{Y' - 1/f}{Y' - 1}. \tag{14}$$

B^{FAC} at 21.2 keV is plotted on Fig. 7.

Finally, the correction factor k_{s} which is used for calibration of an ionization chamber G is determined as:

$$k_{\mathrm{s}} = \frac{B^{\mathrm{FAC}}_{\mathrm{large}}}{B^{\mathrm{G}}_{\mathrm{large}}}. \tag{15}$$

Values of k_{s} evaluated using this method are plotted in **Fig. 9**.

IV. Discussion

In the previous Chapter, it was assumed that X-rays were emitted from a point source. The shape of the X-ray source used in the present study had been measured by a pinhole camera using an X-ray film. It was nearly elliptic and the size was estimated 3 mm × 3.5 mm. If X-rays are emitted only from the area, copper collimators inserted between the X-ray source and the chambers do not shadow the source for all ionization chambers. However, if X-rays are emitted from a wider area, *e.g.*, from a circle area with a diameter more than 17 mm, some part of the X-ray source is shadowed by the copper collimator with a 15 mm diameter hole

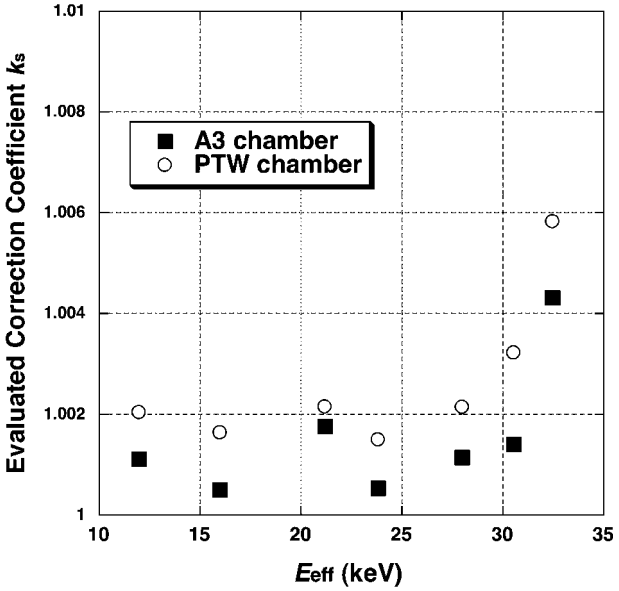

Fig. 9 Evaluated correction factors k_s as a function of E_{eff}

for the PTW chamber. In this case, signal output from the ionization chamber shows large decreases like the results for 30 and 40 mm diameters as shown in Fig. 4.

For the A3 chamber, X-rays from smaller size source are intercepted by the copper collimator because the A3 chamber is larger than the PTW chamber. The experimental result shown in Fig. 3, however, does not show a large decrease like those for the PTW chamber shown in Fig. 4. This is explained from an assumption that the A3 chamber is insensitive for low energy X-rays because the chamber has a thick wall. It is also assumed that low energy X-rays are emitted from the outside of the elliptic area which was measured by an X-ray film; the film may be also insensitive for low energy X-rays due to a slightly thick shading plastic bag.

The evaluated results of k_s shown in Fig. 9 indicate a similar tendency both for A3 and PTW chambers; the k_s slightly increases with an increase of E_{eff}. The present method is based on a simple approximations. In this method, the assumption that the amount of scattered X-rays is proportional to the volume of ambient air which causes scattering may be a rather crude one. This assumption neglects the effect of scattered X-rays from the chamber body, stem and the collimator. Also, the angular dependence of the scattered X-rays is not considered. Moreover, the values of B for 150 mm were obtained by the long-range extrapolation from three data points fitting a quadratic curve.

V. Conclusions

A method has been proposed for calculating the correction factor k_s which is used for calibration of spherical and parallel-plate ionization chambers in a standard X-ray field. Some experiments were carried out to obtain the values of k_s. The results for k_s show similar tendency for A3 and PTW. Although the values of k_s are slightly scattered, we can conclude that about 0.2% correction should be essential for the PTW chamber for X-rays with an energy of E_{eff} less than 25 keV and about 0.3% or greater when the effective energy exceeds 30 keV. Such correction should be taken into account for the calibration of ionization chambers in standard fields.

References

1) J. R. Greening, *Fundamentals of Radiation Dosimetry*, Adam Hilger Ltd., Bristol, London (1985).
2) H. O. Wyckoff, F. H. Attix, *Design of Free-Air Ionization Chambers, National Bureau of Standards Handbook 64* (1957).
3) D. T. Burns, "Sensitivity of X-ray comparisons and calibration to radiation field size," *BIPM CCRI(I)*/**05-04** (2005).
4) A. Nohtomi, N. Takata, C. Kasige, "A correction for scattered X-ray contribution in air kerma calibration," *BIPM CCRI(I)*/**05-29** (2005).